MAPPING THE PRESENCE OF WATER ICE IN PERMANENTLY SHADOWED LUNAR REGIONS USING A TWO-BAND LIDAR. A. E. Parkinson[1] and E. A. Cloutis[1], D. M. Applin[1], and P. J. Mann[1]. [1]Department of Geography, University of Winnipeg, 515 Portage Avenue, Winnipeg, MB, Canada. parkin19@hotmail.com; e.cloutis@uwinnipeg.ca

Introduction: Lunar exploration is of interest because of the possibility of exploitable water ice deposits in permanently shadowed regions (PSRs) [1, 2]. They are also of scientific interest because past lunar exospheric conditions may be preserved in the ice [2].

Multiple lines of evidence and previous studies have suggested that water ice could be present within PSRs [e.g., 3]. They are considered cold traps, reaching temperatures of <120 K, making it possible for water ice to be found within them. Water ice in suitable cold traps can persist for long periods of time. Detecting water ice within these PSRs could possibly be achieved through active reflectance spectroscopy [4].

One concern for detecting the presence of water ice on the Moon is the possibility of dust coverage or mixed ice + regolith [4]. Dust cover thickness, the percentage of ice covered by regolith, and regolith: ice ratio, and how dust and ice are mixed together could all influence the efficiency of detecting water ice [5].

We conducted laboratory experiments to test for how physical properties of ice + powdered lunar rock affect our ability to detect water ice using a two-band lidar system (532 and 1530 nm), which has been proposed as an upcoming ESA-funded mission [6]. We considered water ice: lunar material ratio, temperature, local slope, how the ice and regolith are physically arranged, as well as dust thickness.

Methodology: A lunar highland breccia, meteorite NWA 11444, was reduced to an unsorted powder with a diamond file and alumina mortar and pestle. The sample was subjected to a modified de-rusting process [7]. Reflectance spectroscopy and X-ray diffractometry were used to ensure that the de-rusting process was effective. The ice + NWA 11444 samples were frozen to -40° C. Selected samples were allowed to come to room temperature with continuous spectral collection to determine how long samples could be exposed to ambient conditions and remain frozen. Selected samples were also cooled in a liquid nitrogen bath for similar analysis.

Reflectance spectra (350-2500 nm) were acquired with an ASD Fieldspec Pro HR spectrometer. To simulate a lidar, we used a bifurcated fiber optic bundle, which provided co-aligned incidence and emission (i=e=0°). To measure the effects of local slope on lidar return, all samples except the pure powdered NWA 11444 were tilted 10˚, 20˚, 30˚ and 40˚ to normal. All spectra were measured relative to a calibrated Spectralon panel.

To create ice + regolith mixtures, the powdered NWA 11444 was mixed with appropriate amounts of distilled water to produce various powder + water mixtures. The mixtures were placed into sample cups; these and a mortar and pestle were placed into a freezer overnight and cooled to -40° C. The next morning the samples were crushed within the freezer with the mortar and pestle to ensure the mixtures were homogeneous. The homogenized mixtures were packed into black sample cups and leveled with a glass slide. Once this process was complete the sample cups were returned to the freezer and left overnight to ensure the samples would be at -40° C when measured the next day.

Five ice + rock mixtures were made at 10 wt.% intervals, from 10 to 50 wt.% water ice. Reflectance values at 532 nm, 1530 nm, and a ratio of 1530/532 nm were used to see if water ice abundance could be determined by absolute reflectance or reflectance ratios.

Dust coverage was the final aspect of the experiment to determine the extent lunar regolith coverage affected water-ice detection. Three dust coverages of increasing thickness were used.

Results:

Sample ID	***Description***
NWA 11444 #1	90% Lunar sample 10% Distilled water, unsorted powder multiple incident angles
NWA 11444 #2	80% Lunar sample 20% Distilled water, unsorted powder multiple incident angles
NWA 11444 #3	70% Lunar sample 30% Distilled water, unsorted powder multiple incident angles
NWA 11444 #4	60% Lunar sample 40% Distilled water, unsorted powder multiple incident angles
NWA 11444 #5	50% Lunar sample 50% Distilled water, unsorted powder multiple incident angles
NWA 11444 #6	Loosely applied dust coating allowing a portion of ice to show, unsorted powder multiple incident angles
NWA 11444 #7	Loosely applied dust coating allowing no ice surface to show, unsorted powder multiple incident angles
NWA 11444 #8	Packed applied dust coating pressed down to ensure a flat surface, unsorted powder multiple incident angles
NWA 11444 #9	100 % unsorted powdered NWA 11444, normal incident angle

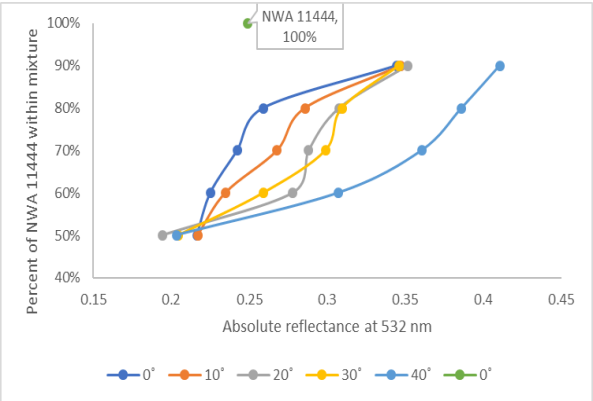

Figure 1. Percentage of NWA 11444 within ice mixture versus absolute reflectance at 532 nm. Shot at varying tilts.

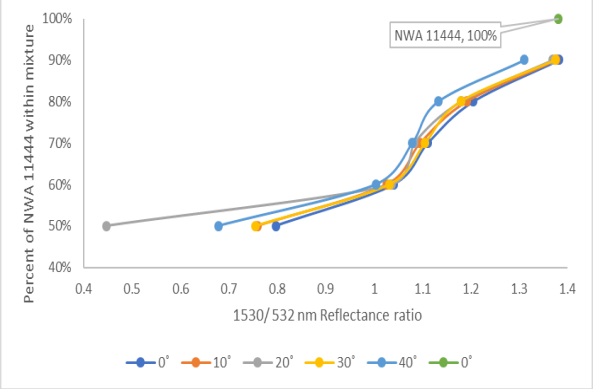

Figure 2. Percentage of NWA 11444 within ice mixture versus 1530/532 reflectance ratio. Shot at varying tilts.

This study supplements previous studies conducted using lunar regolith simulants [8]. As mentioned, our analysis focused on 532 and 1560 nm absolute reflectance and 1530/532 nm reflectance ratio to determine water ice content.

Building on previous research [8], different phase angles were used to examine topographic effects on lidar return. These results were as expected, indicating that slope strongly influences absolute reflectance **(Fig 1, 2)**. Reflectance at 532 nm was highest for the 40˚ slope measurements for a fixed water ice abundance with the smallest spread in values for 50 wt.% water ice. Increases in 532 nm reflectance as a function of water ice content were also greatest for the 40° tilt measurements (**Fig. 1)**.

The 1530:532 nm ratio (**Fig. 2**) results are not as distinctive as the trends seen for 532 nm reflectance (**Fig. 1**). This demonstrates that reflectance ratios are less sensitive to local slopes than absolute reflectance. The 50:50 sample spectra show the greatest difference as a function of tilt. This may be due to the sensitivity of reflectance to surface texture (**Fig. 2**). The other regolith+water ice mixtures show little difference as a function of tilt.

The final aspect of this experiment was as expected for regolith coverage influencing water ice spectra. As the thickness of the dust increases the detection of water ice decreases. Full coverage of ice by dust blocks detection of water ice (second and third dust coverages of NWA 11444 #7 and #8). However, if the dust cover is similar to that of NWA 11444 #6, with incomplete areal coverage by dust, then water ice is detectable. This data can be used to constrain minimum dust thicknesses in regions of no ice detection.

Conclusion: Ice detection is possible using reflectance spectroscopy at 532 and 1530 nm for water ice abundances of 10-50 wt.%. These results indicate that we can determine or constrain whether water ice is exposed at the lunar surface, or covered by a thin dust layer. Combining the observational data with models of ice formation and stability, we can better constrain whether water ice is present on the lunar surface, its abundance, and its areal extent. Absolute reflectance at 532 and 1530 nm, as well as 1530/532 nm reflectance ratios, provide some discrimination in this regard. Additionally, absolute reflectance combined with reflectance ratios may provide constraints on local slopes, which may be important for trafficability. In summary, regions within PSRs that are dust cover-free, or contain more than a few percent water ice can be detected.

Further studies: Further experiments are planned using lunar mare material as well as extending the study to different rock:water ice ratios, dust cover types, and examining the effects of regolith grain size.

References: [1] Nozette S. et al. (2001) *JGR, 106*, 23253–23266. [2] Kruzelecky R. V. et al. (2018) *ICES, 227*, 1–20. [3] Feldman W. C. et al. (2001) *JRG, 106*, 23231–23251. [4] Yoldi Z. et al. (2018) *LPS MMXIX*, Abstract # 2083. [5] Fisher E. A. et al. (2017) *Icarus 292*, 74–85. [6] Kruzelecky R. V. (2018) *COSPAR Scientific Assembly, 42*, Abstract ID B3.1-6-18 [7] Kiddell C. B. et al. (2017) *LPS XLVIII*, Abstract #2397.[8] Cloutis E. A. et al. (2018) *LPS XLIX*, Abstract #2083.

Acknowledgments: This study was supported by grants and contracts from the Canadian Space Agency and the European Space Agency. We also wish to thank the Canada Foundation for Innovation, the Manitoba Research Innovations Fund, the Canadian Space Agency, the Natural Sciences and Engineering Research Council of Canada, and the University of Winnipeg for supporting the establishment and continuing operations of the Planetary Spectrophotometer Facility at the University of Winnipeg.